JOURNAL OF MATERIALS SCIENCE 24 (1989) 3511–3520

Failure processes within ceramic coatings at high temperatures

CHRISTOPHER C. BERNDT
Department of Materials Engineering, Monash University, Clayton, Victoria, 3168, Australia

Plasma sprayed coatings have a complex structure which is produced by the overlaying of many molten or semi-molten particles in the diameter range of 20 to 120 μm. There is a need to characterize the failure behaviour of coatings and this has been carried out by using acoustic emission (AE) methodology.

Coatings of NiCrAlY bond coat with a zirconia–12 wt% yttria overlay were applied to disc-shaped specimens of U-700 alloy. A waveguide of 1 mm diameter platinum was TIG welded to the specimen and allowed it to be suspended in a tubular furnace. The specimen was thermally cycled to 1150° C and the AE monitored.

One method of examining the AE is from the viewpoint of the accumulative count data. It is also convenient to establish the temperatures for "initial" AE and "significant" AE (i.e., the temperature at which 100 counts is exceeded) so that coatings may be compared. Several other analyses have been carried out with the aim of establishing parameters which are related to the crack size and crack population. These studies have been used to postulate types of cracking mechanisms which may occur in plasma sprayed coatings during thermal cycling.

It is shown that microcracking gave rise to a large amount of AE. However, this coating still survived more thermal cycles than a coating which exhibited macrocracking events. Data of this nature will be presented and the results discussed.

1. Introduction

Metals are rarely used without incorporating a protective layer which may be produced by some process such as anodizing, enamelling, painting etc. All coatings are designed with specific applications in mind and for the case of ceramic plasma sprayed coatings the chief advantage is in producing a high wear resistant and good thermal insulator surface layer. These coatings are produced by heating up fine ceramic powders with an intense plasma flame and simultaneously projecting these semi-molten particles against a substrate [1, 2].

A coating consists of many irregular saucer shaped particles which form an interlaced network – much in the form of a complex three-dimensional tile structure. The microstructure is often referred to as "lamellar" to describe the plate-like nature of the coating. Ceramic coatings are usually deposited to a thickness of between 0.5 to 2 mm and are often overlaid onto a plasma sprayed metal (termed the "bond coat") which acts as a compliant layer between the substrate and the ceramic coating. The coating adhesion to the substrate as well as the coating integrity is often explained in terms of the mechanical interlocking of the particles when they solidify. With these factors in mind it can be appreciated that the microstructure of the ceramic coating is not homogeneous and it is thus appropriate to consider it as a composite system.

Cracks within a coating may have a morphology which is either parallel or perpendicular to the substrate surface, Fig. 1. The former mode of cracking eventually leads to loss of the coating by spallation. The coating delamination is most severe close to the bond coat–ceramic interface and failure most commonly occurs just within the ceramic and appears to propagate near to the highly stressed regions of the bond coat asperities [3, 4]. The perpendicular or through-thickness mode may not necessarily contribute to removal of the coating and also may have the beneficial effect of arresting cracks before they cause substantial damage to the overall coating integrity. Microcracking is expected to increase the material toughness since energy which would normally contribute to catastrophic failure will, instead, be dissipated throughout the volume of the coating. It can be seen that the material properties and in particular the failure behaviour of coatings are expected to be dissimilar to the properties of the bulk material.

A major difficulty is to assess the severity of any cracking within the coating. Acoustic emission (AE) methodology lends itself to qualitative measurements on crack activity. It also has the advantage of being a passive (non-interference) technique, measurements can be carried out *in situ* during the testing period and, finally, these measurements may be quantitative if suitable calibration procedures are devised.

2. Acoustic emission methodology

It is not intended to present a complete discussion on AE methodology since this has been covered else-

0022–2461/89 $03.00 + .12

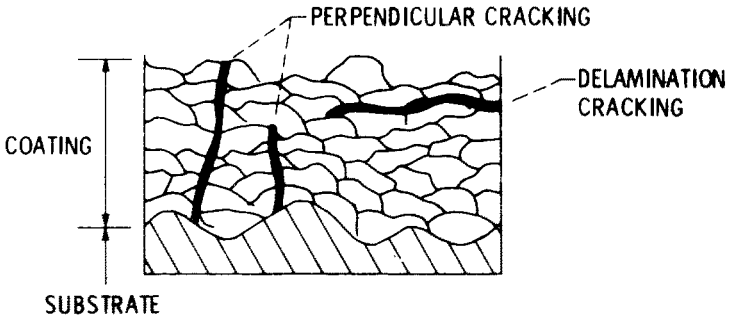

Figure 1 Schematic of crack morphologies in plasma sprayed coatings.

where [5, 6]. However the basic principle is that cracking processes release elastic strain energy which then propagates throughout the body and influences the response of a transducer. In the case of this particular experiment a piezoelectric transducer was used and this gave rise to a sinusoidal decay (or "ring down") in electric voltage for a single AE event. The maximum amplitude of this signal, in simple terms, is characteristic of the magnitude of the cracking events.

Another method of analysing this electrical signal is to count the number of times that it exceeds a certain threshold. This procedure is termed as ring down counting, where the number of counts is proportional to the degree of cracking. The exponential decay of this signal with respect to time, for a single cracking event, is shown in Fig. 2a. The number of counts (N) is taken as the number of times that the signal crosses a certain threshold voltage. The crack growth rate is related to the initial magnitude of the AE elastic wave. However, multiple events which occur simultaneously will also produce a large count.

Consider the case of a cracking event which is monitored at two gain levels. Fig. 2b indicates that this is equivalent to the same signal being monitored at two threshold levels and the difference between N (which is 3 in the example shown in Fig. 2b) is a unique number for each cracking event regardless of the crack size. Table I shows how a simple analysis of these two count rates, which are acquired simultaneously for the same cracking event, can lead to a measurement of the relative crack size and/or the relative number of cracks. These measurements can be used together to ascertain the crack population (an absolute measurement) and crack density (a measurement relative to the unit volume of the material).

There has been some discussion concerning the relevancy of ring down methods in performing AE tests. One major criticism [7] is that the original AE signal is not preserved and thus the modified signal is subsequently processed. On the other hand ring down methodology has a long history [8] of building up useful correlations between the behaviour and structure of materials. The topic of AE is treated in more detail in references [9] and [10]. References [11] to [15] specifically address the application of AE methodology to examining failure processes in thermally sprayed coatings.

3. Experiments

The coatings examined in this study were of ZrO_2–12 wt % · Y_2O_3 which were deposited onto a NiCrAlY bond coat (0.17 mm thick). The substrate was of U-700 superalloy which was in the shape of a 6 mm thick and 13 mm radius disc with well rounded edges. The emphasis of the present work is to illustrate how the AE behaviour of plasma sprayed coatings can be analysed. Two coatings of the same bond coat thickness but different ceramic overlay thickness were selected for analysis. The weights and thicknesses of the plasma sprayed deposits were ascertained during their preparation (Table II). The density of the coating was determined after calculating the volume of the deposit material.

A waveguide of 1 mm diameter platinum was TIG welded to the specimen and allowed it to be suspended into a tubular furnace, Fig. 3. A Dunegan–Endevco 3000 series AE system was used in conjunction with a 0.1 to 0.5 MHz (model D140B) transducer. Two signal amplification levels of 88 and 91 dB were used simultaneously with an aim to carrying out crack size and crack population analyses. The high amplification level was adjusted by thermal cycling an uncoated specimen until no AE activity could be registered. Therefore any AE response could unambiguously be

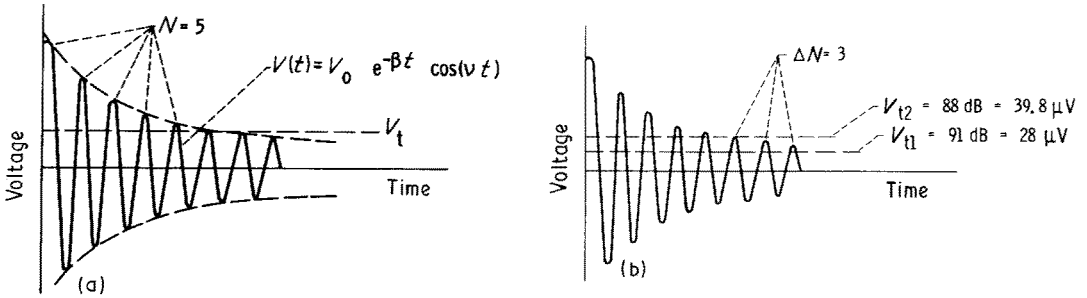

Figure 2 Ideal sinusoidal decay of an acoustic emission signal from one event. (a) Using one gain level, (b) Using two gain levels.

TABLE I Count difference and normalized count difference analyses*

Crack Type	Counts Channel 1	Counts Channel 2	ΔN	$\Delta N/N_1$
Small	10	7	3	0.30
Large	50	47	3	0.06
5 Small	50	35	15	0.30
5 Large	250	235	15	0.06

*ΔN for 1 event has been assumed to be 3 counts for this simple example.

related to cracking processes due to the coating procedure. One of the channels was decreased a further 3 dB so that the relative magnitude of the cracking events could be ascertained. The dead time of the transducer was 100 μsec and the digital updating of the count rate was 0.3 μsec, therefore no aliasing of the counts per event occurred. However, it should be remembered that the AE output from the apparatus is likely to include the superposition of individual AE signals and some of the data is expected to be confounded.

The coatings were thermally cycled for up to 7 cycles to 1150° C and the AE monitored during the specimen cooling. After every cycle the specimen was visually examined at a $\times 10$ magnification and the stage at which macroscopic cracking was observed is indicated as the failure cycle. A major feature of these tests, not addressed by previous work in this area [12, 14, 15] was that the coatings covered 100% of the specimen.

4. Results and analyses

Common methods of displaying AE data are in terms of "count rate" and "accumulative count". The count rate parameter is usually expressed as the number of counts which are measured during a specific time interval which may range from 0.1 sec to the order of hours – depending on the AE activity of the process under study. However for this work another classification will be described where the number of accumulative counts per 20° C increment of temperature are plotted against the temperature range.

Several analyses of the AE data are given in this section. Tests on two samples with different ceramic coating thicknesses are described. Qualitative measures of coating integrity can be gained from an examination of either the count rate or the accumulative count data. It is also intended to show how further information about the cracking behaviour of the coating can be achieved by analysing the AE distributions.

4.1. Accumulative AE data

Significant AE was only detected during specimen cooling and therefore the accumulative counts increase as the temperature decreases. The overall AE behaviour has previously been reported as consisting of two separate distributions [15] – a stochastic response from macrocracking as well as a continuous regime from microcracking. Both of these AE responses must be taken into account when a measure of *significant* cracking is required. The temperature at which significant cracking occurs has been taken as the point where 100 counts has been exceeded. This temperature is quite different from that at which cracking is first observed.

Fig. 4 indicates how the temperatures for significant and initial cracking varies with respect to the thermal cycle. No clear trend is observed for the temperature of the onset of initial failure. However significant failure of specimen 1 was observed to occur at 520 to 650° C whereas specimen 2 failed at 380 to 450° C. It should be cautioned that although specimen 1 failed at a higher temperature during the cooling cycle this does not necessarily indicate a lower susceptability to macroscopic failure.

The accumulative AE per thermal cycle for the two coatings under examination is shown in Fig. 5. It was observed that initial failure of both specimens occurred at about 10 000 to 11 000 counts per thermal cycle when measured at the 91 dB level. After failure was observed the accumulative count either increased or decreased; presumably depending on whether micro- or macrocracking processes, respectively, were the more prominent. The following analysis of the accumulative AE data shows how the relative magnitudes of the cracking processes could be qualitatively discriminated.

The shape of the accumulative AE response with respect to temperature of the samples is shown for selected thermal cycles in Fig. 6. It is observed that the most distinct AE response occurs at temperatures less than about 150° C. The initial accumulative AE response (i.e., at high temperature) of each sample is approximately linear with respect to temperature and the gradient of the corresponding curve in Fig. 6 will now be used to assess the influence of the magnitude of the count per event. Thus it was assumed that macrocracking occurred when the AE count exceeded a certain lower bound which may be considered as a limiting value for the burst emission. All AE counts greater than this specified bound level were discarded and the remaining accumulative AE counts fitted to a straight line with respect to the temperature. This line, therefore, represents the continuous, or microcracking processes which are occurring within the coating.

TABLE II Physical properties of plasma sprayed deposits

Bond Coat				Ceramic Overlay		
Specimen code	Thickness (cm)	Weight (g)	Density ($g\,cm^{-3}$)	Thickness (cm)	Weight (g)	Density ($g\,cm^{-3}$)
1	0.017	1.11	3.4	0.049	5.19	5.0
2	0.017	1.14	3.4	0.040	3.97	4.8

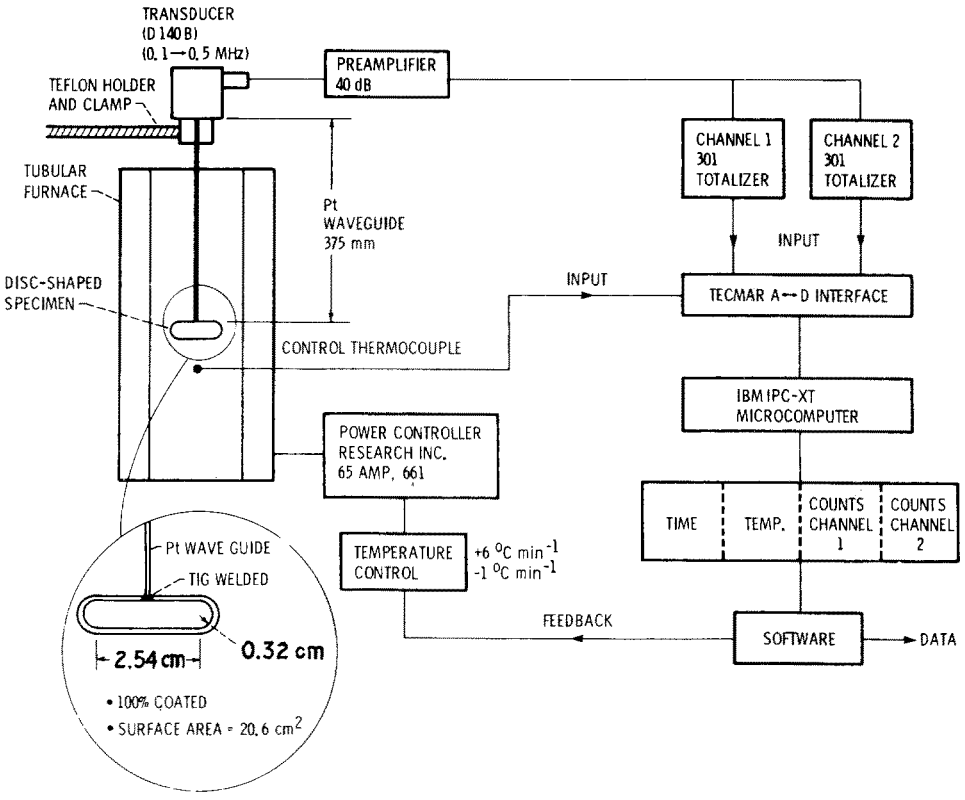

Figure 3 Schematic of experimental arrangement.

The affect of the bound level and thermal cycle number on the gradient of this AE count plotted against temperature relationship will now be studied (Fig. 7).

There is no significant change in the gradient for specimen 2 with respect to the thermal cycle number or AE count bound level (Fig. 7b). The gradient gradually becomes more negative after the second cycle and this indicates that the same cracking processes, even after macroscopic failure was observed at cycle 5, are occurring throughout the thermal cycling but to a greater extent. On the other hand the overall AE activity of specimen 1 is lower since the gradient is a lower negative number. It is also observed that the bound level greatly influences the gradient after the observation of failure at cycle 4. These data show that events with an AE count greater than about 30 correspond to macrocracking whereas less energetic AE events contribute to microcracking processes. The following analyses examine other methods of examining the cracking processes within coatings via AE studies.

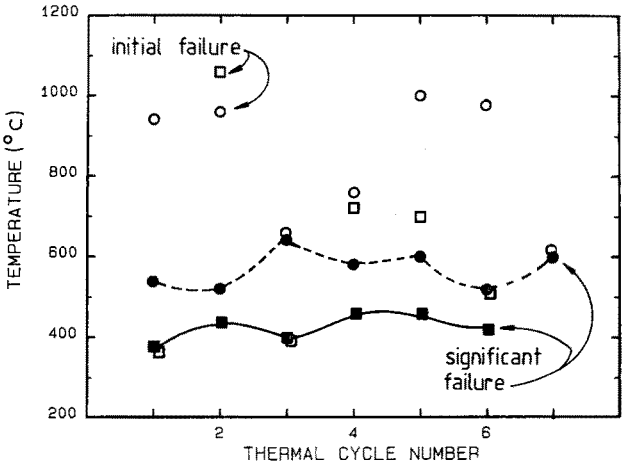

Figure 4 Temperatures for initial and significant cracking of coatings (■ □ specimen 1, ● ○ specimen 2).

4.2. Count difference analysis

Section 2 inferred that the number of cracks may be ascertained by examining the count difference; i.e., the difference in counts between the two amplification levels. These differences have been calculated and are shown as histograms in Fig. 8. A large count difference is related to the simultaneous initiation or growth of many cracks. The frequency of the count differences decreases as the number of simultaneous events (i.e., the count difference) increases. The range of the count difference increased upon thermal cycling and this indicates that the degree of microcracking also increased. The thick coating (indicated by the filled in histogram) displayed lower frequencies of count difference than the thin coating. The thick coating also reveals a decrease in count difference values larger than 20 after failure, and this represents the localization of cracking; i.e., macrocracking. On the other hand the entire distribution of count difference for the thin coating increases after visual failure and microcracking events are still operative.

The count difference analysis indicates that the thin coating fails by microcracking whereas the thick coating microcracks to a lesser extent prior to failing by macrocracking. The analysis shows the relative number of cracks. No absolute value of the crack number can be ascertained because the acoustic damping coefficient of the plasma-sprayed material is unknown. Thus the "count difference" parameter

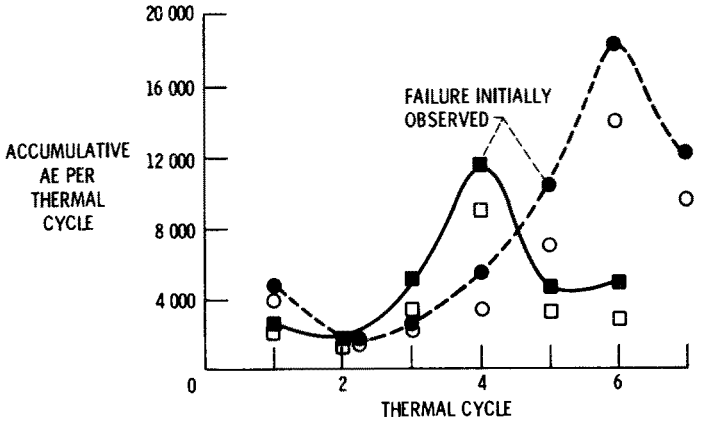

Figure 5 Accumulative AE per thermal cycle for two ceramic coatings. □ ■ thick (5.19 g ceramic), ○ ● thin (3.97 g ceramic). ● ■ Channel 1, 91 dB (× 35 480), ○ □ channel 2 88 dB (× 25 120).

is proportional to the "number of cracks per AE sampling interval".

4.3. Normalized count difference analysis

The magnitude of the AE signal is directly related to the size of the original elastic wave. Therefore the number of counts per AE event is related to the crack growth during the sampling interval. A measurement of the crack growth (or crack size) can be obtained by averaging the count difference over the absolute number of cracks. A more sensitive measurement is obtained if the higher amplified signal is used during the averaging procedure. The function of "1/crack size" was determined since it conveniently lies between 0 and 100%. This simple procedure has been termed as "normalizing" since the result is dimensionless.

The data for the two coatings under scrutiny are shown in Fig. 9. The relative crack size decreases from the left-hand side to the right-hand side of these graphs. On the first thermal cycle the thin coated specimen exhibits more cracking events than the thick coated specimen and all of these crack increments are large. The crack size distributions for both coatings extend to the smaller regime during thermal cycling. After the first cycle the thin coating does not exhibit as high a number of large cracks and the number of AE events for the thick coating increased. The normalized count difference distributions for both coatings appear to be very similar. After failure the thin coating still shows a lot of AE activity, whereas the thick coating exhibits a general decrease over all crack sizes. All of the normalized count difference plots reveal strong periodic peaks in crack sizes of 5 to 10% intervals. It is not known at this stage whether these result from random cracking processes or reflect specific increments of crack growth; for example, crack jumps or one lamellar diameter.

The general view that this analysis presents with regard to the cracking process is that the thin coating sustained many cracks of a large size on the first thermal cycle. This enabled a fine network of cracks to be quickly established during subsequent cycles with the result that the coating was relatively strain tolerant. The thick coating on the other hand did not develop microcracks to the same extent and failure arose from macrocracking phenomenon.

4.4. Crack density function analysis

A more elaborate analysis of the count rate data makes use of a "crack density function" (CDF). This parameter is evaluated by multiplying the count difference and the normalized count difference; and it is a measure of the number of cracks per increment of crack growth. The range in the CDF is quite large (from 1 to 100 000) and therefore in Fig. 10 this function is plotted with logarithmic abscissa. A large value of the CDF infers a large number of cracks for crack growth and, therefore, microcracking. Macrocracking events will, in an alike manner, tend to occur at low values of the CDF.

The thin and thick coatings are initially compared on the second thermal cycle. The coatings are also

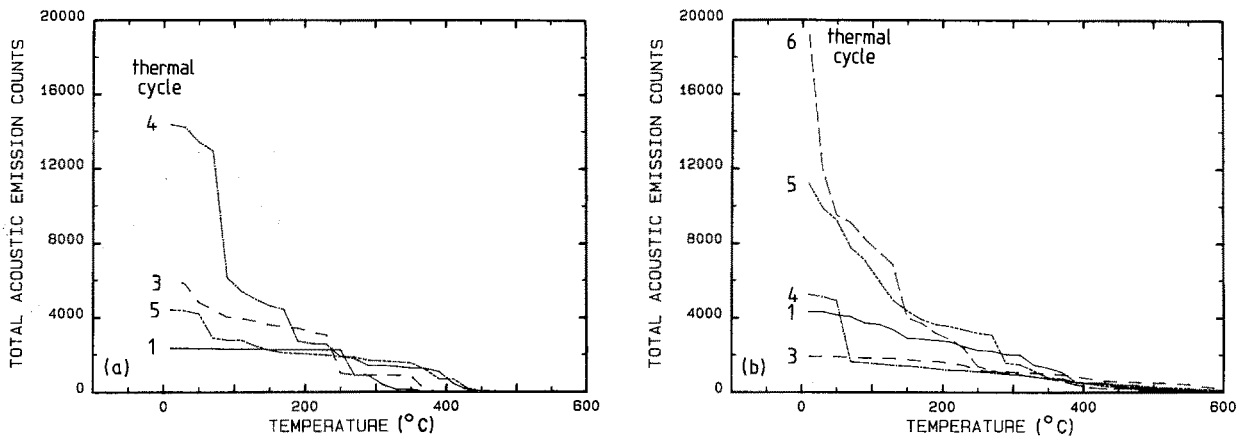

Figure 6 Accumulative counts plotted against temperature data, (a) specimen 1, (b) specimen 2.

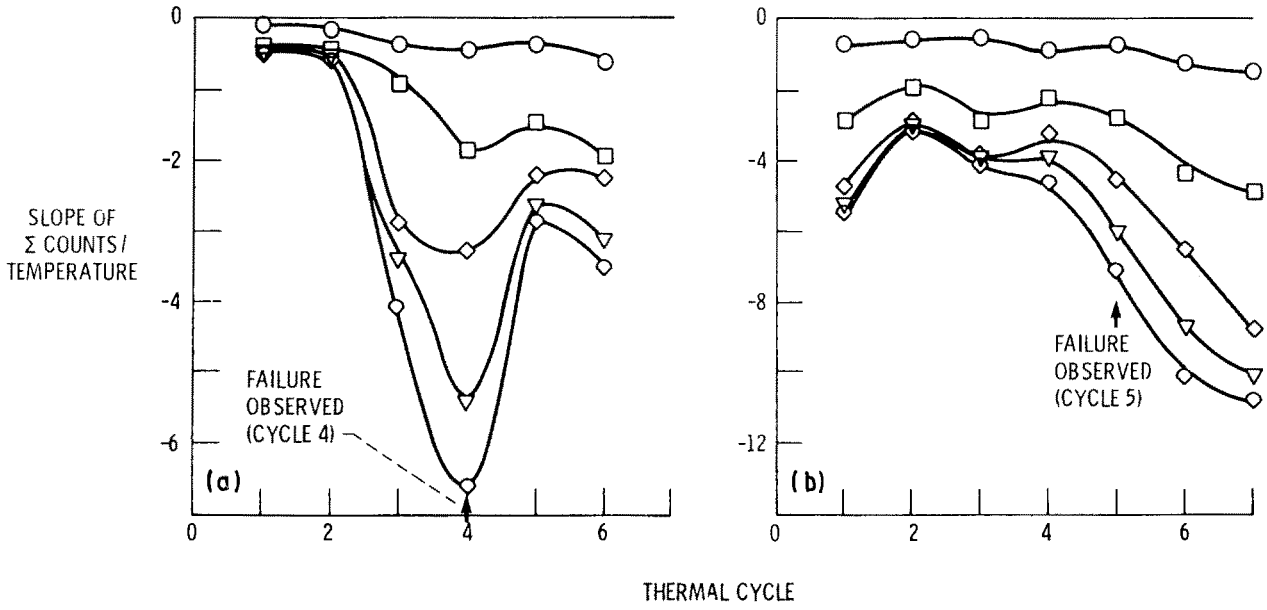

Figure 7 Influence of the bound level and thermal cycle number on the gradient of the accumulative count plotted against temperature data. (a) specimen 1, (b) specimen 2, (bound level in counts per event: ○ 10, □ 30, ◇ 50, ▽ 70, ◇ 90).

compared on the failure thermal cycle and two cycles after failure. It is of interest to note that all of the comparisons up to and including the failure point exhibit very similar total accumulative AE counts. However, the characteristics of the CDF histograms are markedly different and, in general, the thin coating shows a greater frequency at every level of CDF.

The high peak at 100 results from the low amplitude elastic waves which did not excite the low sensitivity amplifier to above the threshold voltage. A second peak is prominent at CDF values of 160 to 250. The shape of the CDF histogram does not change much for the thick coating after the second thermal cycle. On the other hand the thin coating exhibits progressively large increases in high values of the CDF; and this is especially accentuated on and after the failure cycle. It should be emphasized that the thin coating displayed less total counts than the thick coating during most thermal cycles but the CDF was higher. The conclusion reached is that the thin coating failed by progressive microcracking whereas the thick coating gave rise to fewer AE events by macrocracking.

4.5. Distribution analysis

A technique of examining grouped data is to find the nature of the distribution which it forms. In this way it is possible to assign a unique "signature" to the AE response of each specimen which enables direct comparison of the thermal cycling behaviour. The Weibull distribution has wide applicability in the physical world and its form is

$$F(x) = 1 - \exp\left[-\left(\frac{x - x_u}{x_0}\right)^m\right] \qquad (1)$$

where $F(x)$ is the median rank value of the data, x the AE count of each data point, x_u the minimum AE count value, x_0 the characteristic value below which 63.2% of the data lie and m the Weibull parameter (or Weibull modulus).

The distribution is completely described by the

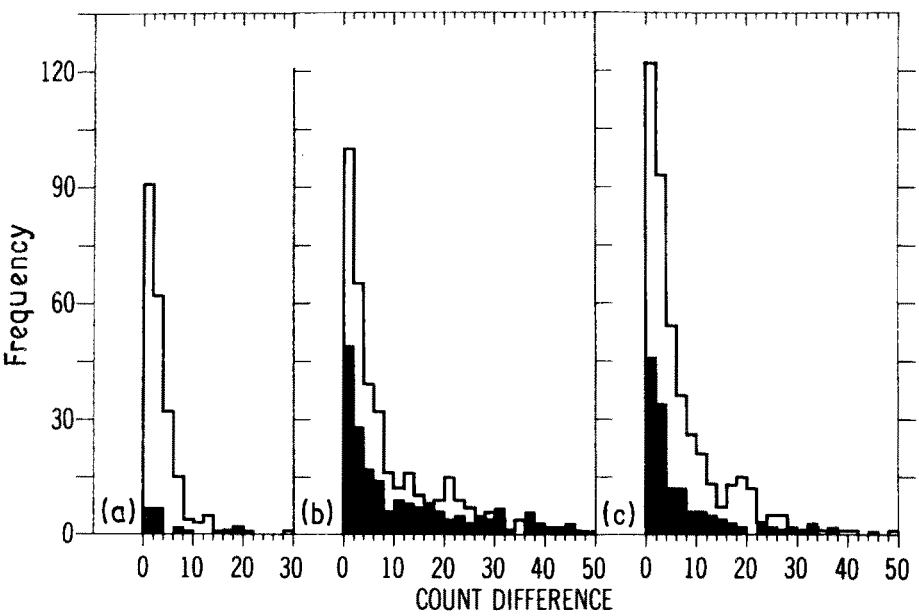

Figure 8 Count difference analysis of coatings. (a) the first thermal cycle (runs 1.1 and 2.1); (b) the failure cycle, (runs 1.4 and 2.5) (c) two cycles after failure (runs 1.6 and 2.7). Note that the "$x.y$" code of the run refers to the specimen number (where x is either 1 or 2) and the thermal cycle number (where y is between 1 and 7). The filled-in histogram refers to specimen 1 whereas the line histogram represents specimen 2.

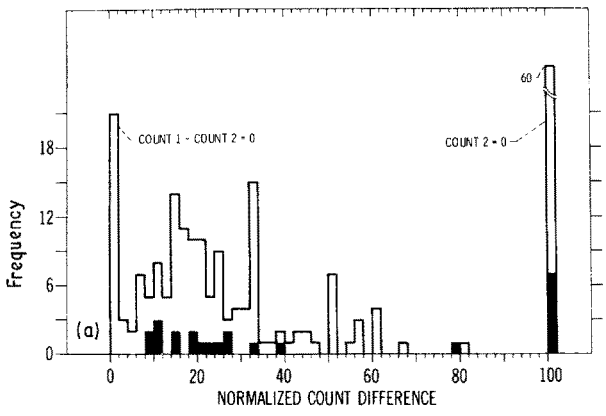

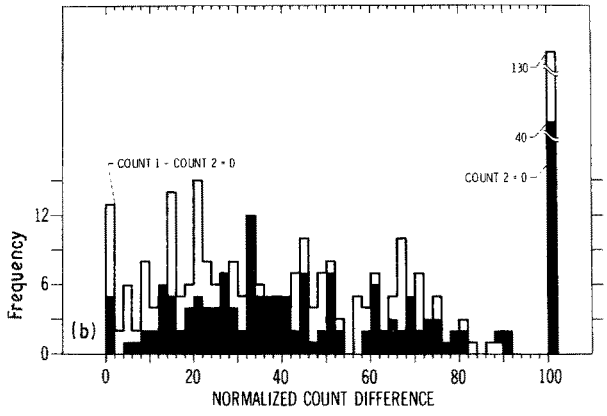

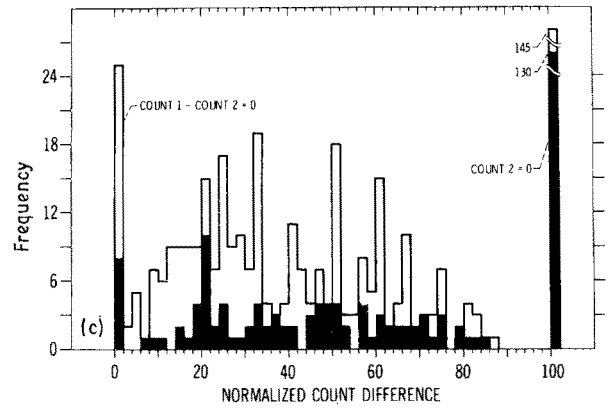

Figure 9 Normalized count difference analysis of coatings. (a) the first thermal cycle (runs 1.1 and 2.1); (b) the failure cycle (runs 1.4 and 2.5); (c) two cycles after failure (runs 1.6 and 2.7). Note that the "$x.y$" code of the run refers to the specimen number (where x is either 1 or 2) and the thermal cycle number (where y is between 1 and 7). The filled in histogram refers to specimen 1 whereas the line histogram represents specimen 2.

three parameters of m, x_u and x_0. The parameter x_u is set to zero since this is the least AE count which is possible in the case of this work.

The count data for each thermal cycle were treated to the above analysis so that x_u and m could be determined. The form of the Weibull plot is shown in Fig. 11 for the first two cycles of specimen 2. A change in each distribution can be observed at values of 50 and 35 counts respectively for cycles 1 and 2. However, the occurrence of monomodal distributions was a more typical result and this assumption was used to find m and x_u values.

The trend of the characteristic AE count parameter with respect to the thermal cycle for each specimen is shown in Fig. 12. The general observations for each specimen are that the characteristic AE count was high on the first cycle, decreased on the second cycle and then increased up to the failure cycle. The characteristic AE count value decreased after the failure cycle. Specimen 1, which had the greater weight of ceramic deposit, also exhibited the highest characteristic AE count values and the greatest change in these values from cycle-to-cycle.

The final way of examining the AE data is by looking at the Weibull parameter ("m") and this is essentially a measure of the distribution shape. A high m value infers that the AE count values are not widely dispersed but grouped about a central value. Both specimens exhibited similar trends in their Weibull parameter behaviour (Fig. 13). The count values occur over a wide range of values during the first thermal cycle but become more centrally located for the

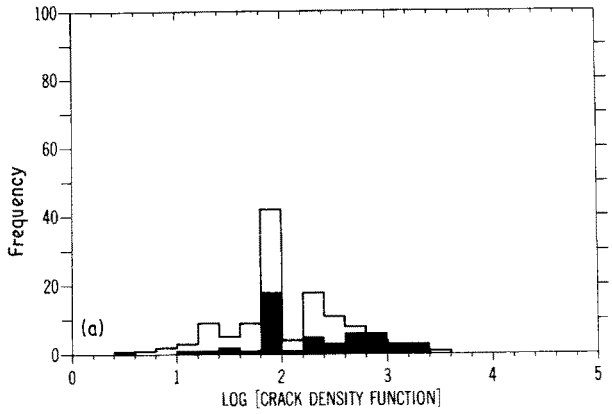

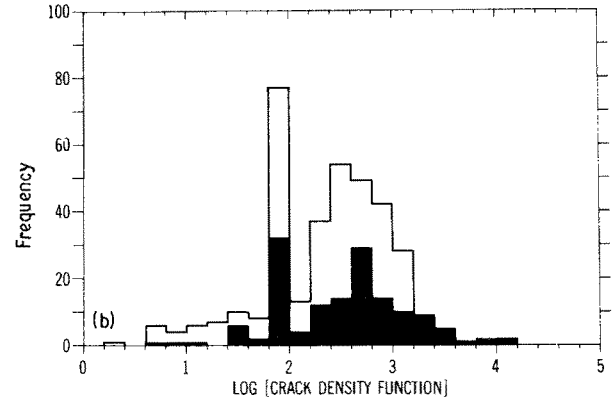

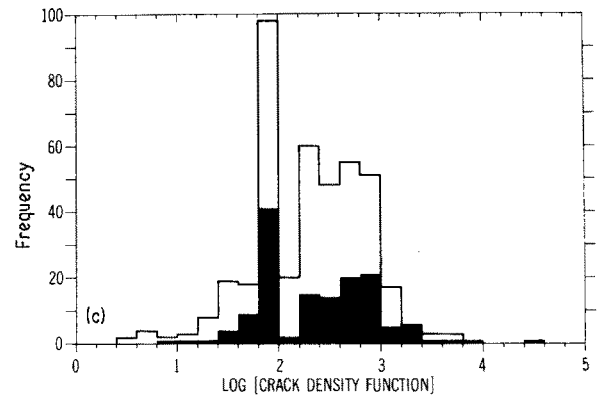

Figure 10 Crack density function analysis of coatings. (a) the first thermal cycle (runs 1.1 and 2.1), (b) the failure cycle (runs 1.4 and 2.5); (c) two cycles after failure (runs 1.6 and 2.7). Note that the "$x.y$" code of the run refers to the specimen number (where x is either 1 or 2) and the thermal cycle number (where y is between 1 and 7). The filled-in histogram refers to specimen 1 whereas the line histogram represents specimen 2.

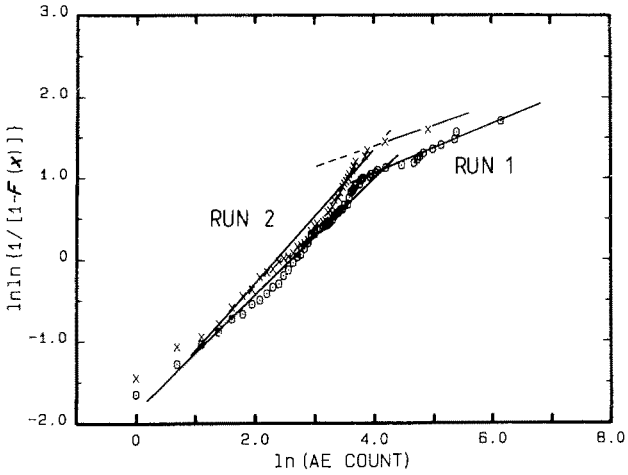

Figure 11 Weibull plot for acoustic emission count data of specimen 2 for two different thermal cycles.

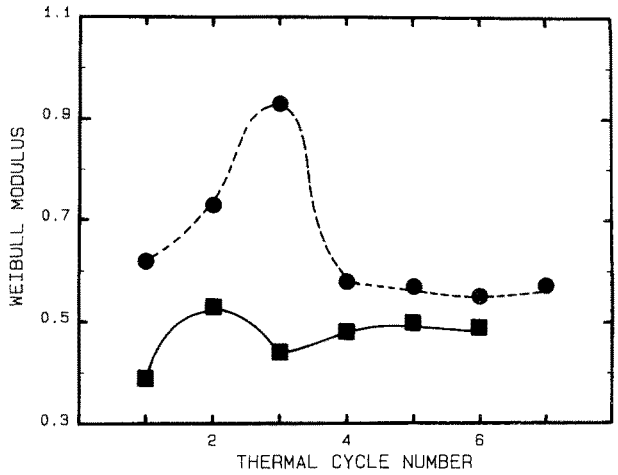

Figure 13 Weibull parameters for plasma sprayed coatings subjected to thermal cycling, (■ specimen 1, ● specimen 2).

second and third thermal cycles. Prior to observed failure the distribution of specimen 2 is again altered to a wide range of AE counts whereas the m parameter of specimen 1 does not change significantly. The physical inference is that specimen 2 cracks significantly at cycle 3 from events which are all very similar in terms of AE count (i.e., microcracks); however, on cycle 4 there is a large variety of cracking processes (i.e., including macrocracks) and this is reflected by a wide range in the AE count data. Specimen 1 on the other hand always exhibits a large variability in AE count range and never any AE processes which are concentrated within a narrow band of activity.

5. Discussion

Acoustic emission methodology often leads to the acquisition of much data which must be interpreted to reveal trends (of a numerical or qualitative nature) which are correlated to materials properties. An important assumption which must always be remembered is that cracking processes within the plasma sprayed coating give rise to AE. In the case of these experiments the threshold voltage (or amplification level) was adjusted so that only effects which arose from the thermal cycling of the coating produced AE. Thus any oxidation of the substrate, which would produce AE, is not included in the results reported in the present work. Furthermore oxidation effects, other than processes which would normally occur by diffusion through the coating to the substrate, have been avoided by completely coating the substrate over its entire surface. Another experimental factor which has been closely controlled is the careful rounding of all substrate edges, otherwise, these would be expected to be the preferred failure locations.

An important consideration concerns the method of using ring down counting for the measure of AE response. The major shortcoming is that the initial AE waveform is not reproduced by detecting it with a piezoelectric transducer. The electrical response from the AE event is produced from its initial strain transient and this decays with time. Therefore, to a certain degree, the ring down count is an artefact of the transducer response to the AE event. It is generally true that large cracking events will produce a large ring down count and in this way the ring down count per event, or the accumulative ring down count, are measures of the cracking magnitude and degree of cracking respectively. Another consideration to keep in mind is that an ideal sinusoidal decay signal is very rarely encountered. Thus the focus of any interpretation of the AE data reported in this paper should not be on any individual AE event but should be centred on trends of a general nature.

The two coatings under examination were produced with approximately the same bond coat thickness (0.017 cm) and weight of material (1.11 to 1.14 g). The thickness of the ceramic coatings were nominally different but it should be remembered that the error of these measurements is about ± 0.006 cm [16]. However despite this ambiguity it is known that coating 1 had 23% more deposit material than coating 2. Also the ceramic coating densities were calculated as 4.8 to 5.0 g cm^{-3} which agrees well with independently measured values in the literature [16]. However the densities of the bond coats were calculated as 3.4 g cm^{-3} which, despite error corrections from the thickness measurement, disagree with the literature values of 6.9 to 7.4 g cm^{-3} [16]. Thus the bond coats which were studied in this work are not typical of the usual relatively dense coatings. Regardless of the

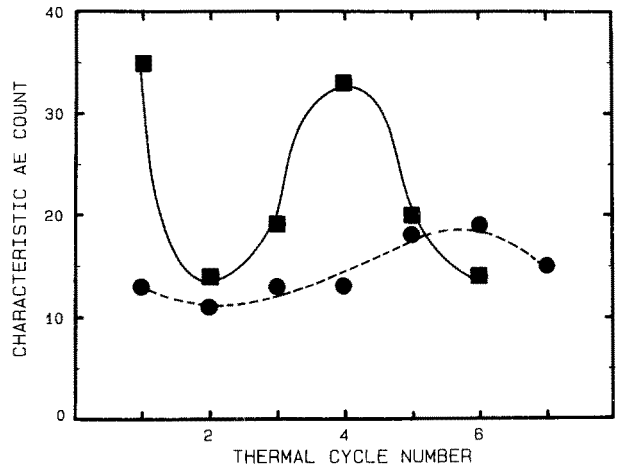

Figure 12 The characteristic acoustic emission count of plasma sprayed coatings subjected to thermal cycling. (■ specimen 1, ● specimen 2).

above shortcomings the two coatings can be thought of as virtually identical except for the weight of the ceramic overlay. Both coatings were produced in an identical fashion so the weight difference corresponds to a real difference between the ceramic coating thicknesses. Therefore, in this light, it is convenient to consider that coating 1 has a "thick" ceramic overlay whereas coating 2 is "thin".

A major aim of the AE tests has been to examine the coating integrity with respect to temperature. There is a need to establish the cracking behaviour of coatings and, more importantly, to define the conditions which constitute favourable or detrimental cracking with respect to the overall coating adhesion and performance. The accumulative AE count and accumulative AE bound level analyses, Figs 5, 6 and 7, closely parallel each other. It is shown that large AE counts result from many simultaneous cracking events rather than from large individual cracks. Another feature is that the thin coating produces almost double the amount of AE than the thick coating during the first thermal cycle. However, after the first cycle and up to the failure cycle the AE response of the thin coating is less than that which is exhibited by the thick coating.

It is difficult to relate the temperature at which AE is first observed to any of accumulative AE distributions. This is most probably because these emissions are of a mixed stochastic–continuous nature and therefore are, to a certain degree, a response to the relief of internal stresses within the coating–substrate system. The temperature of this very first emission is not easy to predict as can be ascertained by the variable nature of the accumulative AE curves during the initial cooling. The figure of merit that was used to determine a significant cracking temperature averages the various AE responses so that almost constant temperatures were observed (Fig. 4). On application of this measure for cracking it is seen that the thin coating reaches the significant value at about 550° C whereas the thick coating reaches the same significant value at 420° C. It is of major importance to emphasize that the coating which started cracking at the higher temperature also produced less AE per thermal cycle up to the failure cycle (disregarding cycle 1). This inverse correlation between high temperatures for significant cracking and a low total AE infers that the crack growth rate (or possibly crack nucleation) with respect to temperature is less for the thin coating.

The "crack growth function" is calculated from the count difference values which have been normalized with respect to the larger count value. The accumulative reciprocal of this function may be considered a measure of the total damage (or crack growth) within the coating. Fig. 8 indicates that there is a large difference in the failure behaviour of the two coatings examined and that these differences are not as distinctly shown in Figs 5 and 7. For example the coating with the less weight of deposited ceramic (specimen 2) exhibited a greater magnitude of crack growth than specimen 1 on all thermal cycles and this extended up to a factor of about 9 on the first thermal cycle. Coupled with this is the accumulative AE data of specimen 2 which is less than that for specimen 1 for thermal cycles up to the failure point (disregarding the first thermal cycle). Therefore there is an inference that specimen 2 failed by many small cracking events in comparison to specimen 1.

Another feature of Fig. 8 to be considered is the general trend of the crack growth function curve with respect to the thermal cycle. Specimen 1 displays an increase in the crack growth function until the failure cycle (cycle 4) at which point the crack growth parameter decreases. On the other hand specimen 2 shows a decrease in crack growth after the initial thermal cycle and then a large increase at failure (cycle 5) which increases further with the next cycle (cycle 6).

Another method of studying coating behaviour is by classifying the AE distributions. The AE data for each thermal cycle was fitted to the Weibull distribution and the parameters of m and x_u were used to characterize the coating. The "characteristic AE count" shows that specimen 2 behaves at a lower level of AE activity than specimen 1 and this low activity (about 12 counts per event) is probably related to microcracking rather than macrocracking processes. The first thermal cycle of specimen 1, on the other hand, exhibited large AE counts (characteristic value of 35 counts per event) and this represents a greater degree of cracking. Another feature of both distributions is that observable failure of the specimen occurred near to the maximum of the characteristic AE count and on subsequent thermal cycles the characteristic AE count decreased. The shape of the distribution is given by the Weibull parameter. A high value corresponds to a distribution where the values are centrally located whereas "m" is low if the AE counts are dispersed over the range. Specimen 2 exhibited distributions with a greater m than specimen 1 (Fig. 13) and this behaviour infers that the cracking processes are of a similar character.

Mechanisms of failure may be postulated to account for the relative difference in AE behaviour between the two specimens. Specimen 1 progressively failed by a few large scale cracks (macrocracks) which coalesced at the point of catastrophic failure so that further cracking was localized. Specimen 2 exhibited very many small cracks (microcracks) on the first thermal cycle and these caused a reduction in the extent of cracking on the following cycles; most probably by crack interaction mechanisms. At the failure point (cycle 5) there is activity generated by new cracks being formed and this process continues after the failure cycle (i.e., during cycle 6).

One final point concerns the significance of the life-times which are reported for these tests. For example it may be thought that an absolute difference of one thermal cycle corresponds to virtually equivalent life-times. However an alternative view point is that the relative difference in lifetimes is 20 to 25%; and this is considered quite a significant change in other thermal tests such as burner rig or quenching experiments. Regardless of these arguments it should be emphasized that the major thrust of this work has been describing and discussing the various AE distributions of several specimens. In the case of these experiments it is shown how the thin coating failed by

a different mechanism than the thick coating. Another caution concerns the question of replicating results. In this work each test must be considered quite unique. Even if specimens could be superficially identical there is always the doubt that some microstructural feature(s) will cause an "untypical" mechanism of failure and hence lead to a variation in the AE response. Thus the aim of this work has been to identify and classify trends in the AE behaviour of plasma sprayed coatings.

6. Concluding remarks

Acoustic emission methodology has been used to study the failure processes of plasma sprayed NiCrAlY + ZrO_2–12 wt · % Y_2O_3 coatings. Several techniques of analysis have been used to describe the mechanism of failure in relative terms of the number of cracks and their activity, i.e., their initiation or growth. The temperature at which significant crack activity commences has been defined and found to be inversely related to the accumulative count. Thus the coating which exhibited the higher significant temperature also revealed a lower total accumulative count. The cracking at high temperatures may relieve the stresses that would otherwise be detrimental at a lower temperature.

These studies have focussed on examining the cracking behaviour of plasma-sprayed coatings by acoustic emission methods. Two specimens, identical except for the ceramic coating thickness, have been studied by repeated thermal cycling to 1150° C. The analyses are limited to a certain extent by the non-ideal nature of the AE response which is, in turn, manifested by non-sinusoidal decay of the electrical signal from the transducer. Another basic assumption is that the AE signals from separate events are not superimposed and thereby confounded. It is expected that the same trends in the AE data would be observed if these errors were taken into account since the results would still be distributed about the same mean values.

The difference in counts between the two amplifiers is used as a qualitative measure for the number of cracking events. The count difference analysis provides a means for relative estimation of the number of active cracks. The crack size can also be examined by studying the normalized count difference, and a crack density function is derived which incorporates the size and number of cracks. Finally, a Weibull distribution analysis is used to provide details concerning the relative contributions of macro- and microcracking events. Some of these analyses use the same raw data but process them by different mathematical means. All these analyses provide insights into the thermally induced failure processes within coatings.

Acknowledgements

This work has been supported by NASA-Lewis Research Center and the Australian Research Council.

References

1. I. A. FISHER, *Int. Met. Rev.* **17** (1972) 117–129.
2. D. A. GERDEMAN and N. L. HECHT, "Arc Plasma Technology in Materials Science", (Springer, New York, 1972).
3. R. A. MILLER and C. E. LOWELL, *Thin Solid Films* **95** (1982) 265–273.
4. G. C. CHANG and W. PHUCHAROEN, in Thermal Barrier Coatings Workshop, May 21-22, 1985, (NASA-Lewis Research Center, Cleveland, Ohio, 1985) pp. 116–126.
5. J. R. MATTHEWS, "Acoustic Emission", (Gordon and Breach, New York, 1983).
6. R. G. LIPTAI, D. O. HARRIS and C. A. TATRO, ASTM STP505, (American Society for Testing and Materials, Philadelphia, 1972).
7. R. E. GREEN, Jr, in Symposium proceedings of "Novel NDE Methods for Materials", (Metallurgical Society of the AIME, Warrendale, Pennsylvania, 1983) pp. 131–139.
8. T. F. DROUILLARD, "Acoustic Emission: A Bibliography with Abstracts", (Plenum, New York, 1979).
9. H. N. G. WADLEY, C. B. SCRUBY and J. H. SPEAKE, *Int. Met. Rev.* **25** (1980) 41-64.
10. R. W. HARRIS and B. R. A. WOOD, *Metals Forum* **5** (1982) 210-215.
11. D. ALMOND, M. MOGHISHI and H. REITER, *Thin Solid Films* **108** (1983) 439-447.
12. N. RAVI SHANKAR *et al., Amer. Ceram. Soc. Bull.* **62** (1983) 614-619.
13. C. C. BERNDT, *ASME J. Eng. for Gas Turbines* **107** (1985) 142-146.
14. C. C. BERNDT and H. HERMAN, *Thin Solid Films* **108** (1983) 427-437.
15. C. C. BERNDT and R. A. MILLER, *ibid.* **119** (1984) 173-184.
16. S. STECURA, Effects of Plasma Spray Parameters on Two-Layer Thermal Barrier Coating System Life", NASA TM81724, March 1981.

Received 5 July
and accepted 8 December 1988